Dynamic transition from Mott-like to metal-like state of the vortex lattice in a superconducting film with a periodic array of holes

Indranil Roy,[1] Prashant Chauhan,[2] Harkirat Singh,[1] Sanjeev Kumar,[2] John Jesudasan,[1] Pradnya Parab,[2] Rajdeep Sensarma,[1] Sangita Bose,[2,*] and Pratap Raychaudhuri[1,†]

[1]*Tata Institute of Fundamental Research, Homi Bhabha Road, Colaba, Mumbai 400005, India*

[2]*UM-DAE Center for Excellence in Basic Sciences, University of Mumbai, Vidhyanagari Campus, Mumbai 400098, India*

(Received 22 September 2016; revised manuscript received 3 February 2017; published 22 February 2017)

We show that under an ac magnetic field excitation the vortex lattice in a superconductor with a periodic array of holes can undergo a transition from a Mott-like state where each vortex is localized in a hole, to a metal-like state where the vortices get delocalized. The vortex dynamics is studied through the magnetic shielding response which is measured using a low-frequency two-coil mutual inductance technique on a disordered superconducting NbN film having a periodic array of holes. We observe that the shielding response of the vortex state is strongly dependent on the amplitude of the ac magnetic excitation. At low amplitude the shielding response varies smoothly with the excitation amplitude, corresponding to the elastic deformation of the vortex lattice. However, above a threshold value of excitation the response shows a series of sharp jumps, signaling the onset of the Mott-to-metal transition. A quantitative analysis reveals that this is a collective phenomenon which depends on the filling fraction of vortices in the antidot lattice.

DOI: 10.1103/PhysRevB.95.054513

I. INTRODUCTION

Understanding the vortex dynamics in strongly pinned type II superconductors is of paramount importance both from fundamental and practical points of view. On the one hand, the vortex lattice (VL) provides a versatile model system to understand the interplay of interaction and pinning in a periodic solid [1,2]. On the other hand, the collective dynamics of the VL determines the critical current, which dictates the limit of the applicability of the material in low loss devices. Of particular interest are superconductors with a periodic array of holes, i.e., antidot arrays, which act as strong pinning centers for the flux lines [3–8]. Here, besides the overall confining potential created by the shielding supercurrent, each vortex experiences two kinds of forces: the nearly field independent confining potential of the antidot and the field dependent confining potential caused by the repulsive interaction of surrounding vortices. At matching fields, corresponding to an integer number of vortices in each antidot, each vortex gets tightly confined in a cage formed by the neighboring vortices. This gives rise to a pronounced oscillatory response of the superconductor with the magnetic field, known as the vortex matching effect (VME), which manifests as oscillations in magnetoresistance close to the superconducting transition temperature (T_c), with a period corresponding to the first matching field (H_m). It has been suggested that when thermal fluctuations are not large enough to overcome the combined confinement caused by the antidot and the intervortex interactions, the vortex state close to the matching field mimics that of a Mott insulator [9], where each vortex is localized around the antidot. Early evidence of the vortex Mott state in superconductors with periodic pinning [10,11] was further confirmed from detailed measurements of the compressibility of the vortex lattice [12]. Recently, a transition of this vortex Mott insulator state to a metallic state, where vortices become delocalized, as a function of magnetic field or induced by an external current [13] has also been reported.

In this paper, we investigate the dynamic response of the VL in a disordered superconducting NbN film with an antidot array, when subjected to an ac magnetic field with a varying amplitude. We focus on the low-temperature limit ($T \ll T_c$) where thermally excited vortex motion does not play a significant role. The usual transport measurements, i.e., resistivity and critical current, conventionally used to study VME cannot be used here, since they are restricted to temperatures [14] very close to T_c. To overcome this difficulty, we developed a "two-coil" mutual inductance technique [15] which can extend these measurements to well below T_c. Here, the superconducting film with an antidot array is sandwiched between a quadrupolar primary coil and a dipolar pickup coil. When a small ac current (I_{ac}) is passed through the primary, the flux tubes undergo oscillatory motion about their equilibrium position, thereby inducing a voltage in the secondary. The VME reflects in the periodic modulation of the magnetic shielding response. This is measured from the real and imaginary parts of the mutual inductance, $M'^{(\prime\prime)}$, which are related to the compressibility of the VL and the dissipation inside the superconductor, respectively. Here, we study the shielding response as a function of I_{ac}, which is proportional to the ac magnetic field. The central result of this paper is that as I_{ac} is gradually increased, the VL undergoes a transition from a Mott-like to a metal-like state, at a characteristic I_{ac} value which is much smaller than the depinning threshold for an isolated vortex from the antidot, showing that this is a collective phenomenon dominated by vortex-vortex interactions. Furthermore, the I_{ac} at which this transition happens is strongly dependent on the filling fraction of the vortex lattice and is lowest at H_m when the VL is most rigid. Interestingly this is opposite to the behavior inferred from critical current measurements [5] close to T_c.

*sangita.bose@gmail.com

†pratap@tifr.res.in

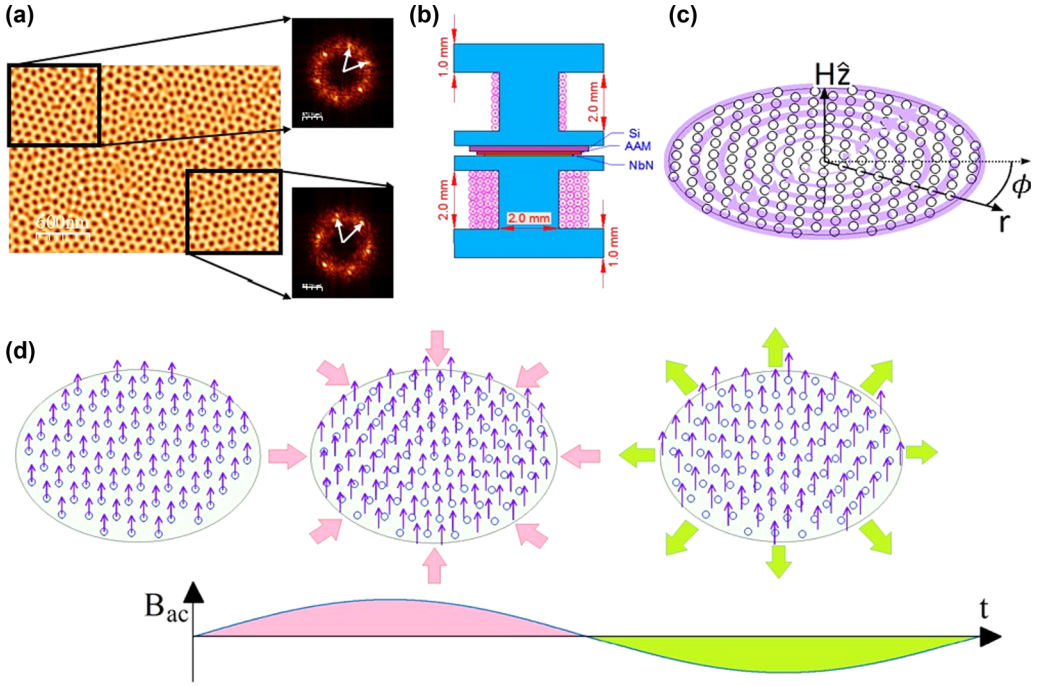

FIG. 1. (a) Scanning electron micrograph showing the NbN film with an antidot array. The panels on the right show the Fourier transforms of the areas bounded in the respective boxes. The six spots in the Fourier transform show local hexagonal ordering. (b) Schematic diagram of the two-coil mutual inductance setup. (c) Schematic diagram showing the circulating ac supercurrent setup in a circular film with an antidot array due to the alternating magnetic field from the primary coil. The width of the circles is proportional to the amplitude of $J_S^{\rm ac}$. (d) Schematic description of the compression and rarefaction of the VL in one cycle of the alternating magnetic field. The leftmost panel shows the VL without an external ac field.

II. SAMPLE DETAILS AND MEASUREMENT SCHEME

Sample. The sample used in this study consists of a 3-mm-diameter disordered NbN film with a thickness $t \sim 25$ nm, grown using reactive magnetron sputtering on a nanoporous anodic alumina template (AAM). Details of the synthesis and characterization have been reported earlier [16]. The condition for observing VME is that the intervortex repulsive force should be a non-negligible fraction of the individual pinning force by the antidot. While close to T_c the divergence of the Ginzburg-Landau coherence ($\xi_{\rm GL}$) length ensures that this condition is easily satisfied [15], the observation of VME at $T \ll T_c$ requires careful tuning of the material parameters. In NbN, the introduction of disorder (in the form Nb vacancies) decreases the strength of individual pinning through an increase [17] in $\xi_{\rm GL}$ and a decrease in the superfluid density [18,19], making this condition achievable down to low temperatures. Consequently, we perform our measurements on a disordered NbN film with $T_c \sim 4.21$ K, for which vortex matching effects are observed down to the lowest temperature of our measurement (1.45 K). Scanning electron micrographs (SEMs) of the film [Fig. 1(a)] obtained after deposition show pores with an average diameter $d = 46$ nm, nominally arranged in a hexagonal pattern with an average lattice constant $a = 107$ nm. However, the hexagonal ordering is not perfect. A two-dimensional (2D) Fourier transform of different areas [20] of the SEM image show six symmetric diffraction spots, but misoriented with respect to each other [right panels in Fig. 1(a)]. This shows that, in addition to imperfections in the position of individual holes, the nanopores also form domains, misoriented with respect to each other, similar to a polycrystal.

Measurement. The schematics of our two-coil mutual inductance setup is shown in Fig. 1(b). The quadrupolar primary coil has 28 turns with the upper half wound in one direction and the lower half wound in the opposite direction, producing a peak field of 7 mOe/mA. The dipolar secondary coil consists of 120 turns wound in four layers. To measure the mutual inductance, a small sinusoidal excitation current ($I_{\rm ac} \sim 1-15$ mA) with a frequency $f = 31$ kHz is passed through the primary and the in-phase (V') and out-of-phase voltage (V'') induced in the secondary is measured using a lock-in amplifier. The real and imaginary parts of mutual inductance are defined as $M'^{(\prime\prime)} = V''^{(\prime)}/(2\pi I_{\rm ac} f)$, such that M' and M'' correspond to the inductive and dissipative response of the sample. The two-coil assembly is placed in a cryostat fitted with a superconducting solenoid capable of generating a dc magnetic field ($H \perp$ film plane) up to 90 kOe.

To understand what the quantities M' and M'' relate to, we note that the magnetic field produced by the primary coil will generate a *coarse grained averaged* time varying circulating supercurrent of the form $\boldsymbol{J}_S^{\rm ac}(\boldsymbol{r},t) = J_S^{\rm ac}(r)\sin(\omega t)\widehat{\phi}$ in the superconducting film [Fig. 1(c)], which from symmetry considerations will be zero at the center of the sample and will increase towards the periphery. (Here we ignore the pattern of the supercurrent on a shorter length scale due to the presence of the antidots.) This will apply a radial oscillatory force (per unit length) on each vortex given by $\boldsymbol{F}_{\rm ac} = \boldsymbol{J}_S^{\rm ac} \times \hat{z}\Phi_0 = J_S^{\rm ac}(r)\sin\omega t\,\Phi_0\hat{r}$, causing each vortex to oscillate about its

equilibrium position. Thus, as a first approximation, the effect of the ac excitation is to produce an oscillatory compaction and rarefaction of the VL with the vortex at the center of the sample remaining in its equilibrium position [Fig. 1(d)]. This is equivalent to a periodic change in the flux density which will produce an induced voltage in the secondary coil. Thus M' is a measure of the compressibility of the VL. The amplitude of the imaginary part $-M''$, on the other hand, is related to the dissipation in the superconductor. At small ac excitations, when each vortex undergoes small oscillations about its equilibrium position, this dissipation arises from Bardeen-Stephen loss inside the superconductor surrounding the antidot. However, when the excitation is large enough to induce vortex hopping from one antidot to the next, the dissipation comes predominantly from the 2π phase slips in the intervening superconductor separating the two antidots.

III. RESULTS AND DISCUSSION

Figure 2 shows the $M'-H$ scans recorded at different temperatures between 3 and 1.45 K with $I_{ac} \sim 5$ mA. M' shows a dip at multiples of 2.37 kOe, consistent with the expected matching field, $H_M = \frac{2\Phi_0}{\sqrt{3}a^2}$, where Φ_0 is the flux quantum. The dips in M' show that the VL becomes more rigid at the matching fields, consistent with the description of a vortex Mott state [9,21]. Decreasing the temperature has two effects: First, the overall magnetic screening response increases, and second, the minima in M' at matching fields become less pronounced. At a qualitative level, both these effects can be understood from the temperature variation of the coherence length ξ_{GL} and the magnetic penetration depth λ of the superconductor as outlined in Ref. [15]. The first effect can be understood from the fact that the pinning potential and therefore the individual pinning force $F_p \sim \frac{\Phi_0^2}{4\pi\mu_0\Lambda\xi_{GL}}$, where $\Lambda(=2\lambda^2/t)$ is the Pearl's penetration depth and μ_0 is the vacuum permeability. Assuming the dirty Bardeen-Cooper-Schrieffer (BCS) relation $\frac{\lambda^{-2}(T)}{\lambda^{-2}(0)} = \frac{\Delta(T)}{\Delta(0)} \tanh(\frac{\Delta(T)}{2k_BT})$

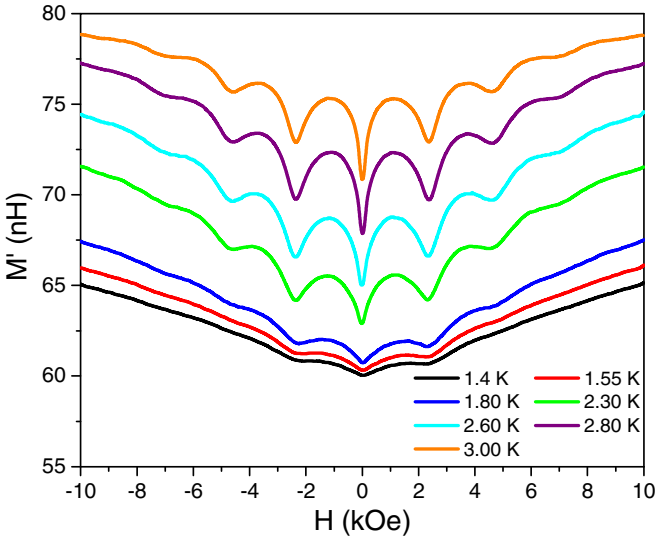

FIG. 2. Variation of M' as a function H at different temperatures with $I_{ac} \sim 5$ mA. VMEs manifest as minima in M' at matching fields.

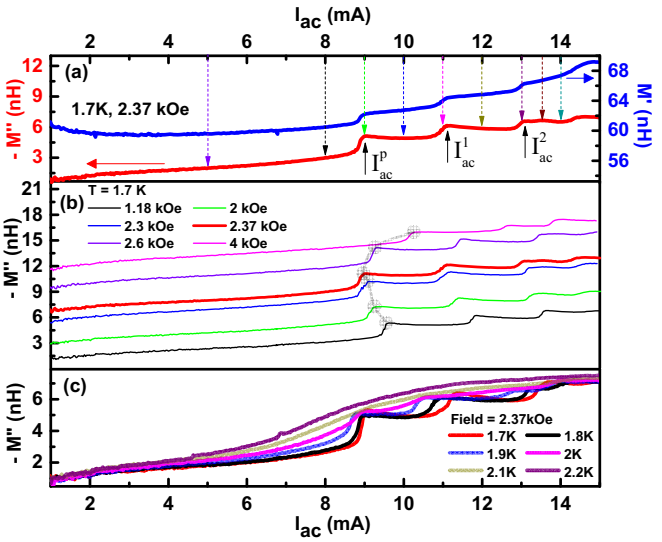

FIG. 3. (a) M' and $-M''$ as a function of I_{ac} for fixed values of the dc magnetic field $H = H_m = 2.37$ kOe at 1.7 K. Both quantities show a series of jumps above $I_{ac} \sim 8.8$ mA. The vertical dashed arrows correspond to I_{ac} values for which $M'-H$ and $-M''-H$ are plotted in Fig. 5. (b) $-M''$ as a function of I_{ac} for different H below and above H_m at 1.7 K; for clarity, each successive curve for $H>1.18$ kOe is shifted upwards by 2 nH. The gray curve show the locus of I_{ac}^p. (c) $-M''$ as a function of I_{ac} for $H = 2.37$ kOe at different temperatures; above 2 K the sharp jumps transform into a smooth variation.

(where Δ is the superconducting energy gap and k_B is the Boltzmann constant), $1/\lambda^2$ increases by 30% when we cool the sample from 3 to 1.45 K. Thus, at low temperatures, the vortex lattice becomes more strongly pinned, thereby increasing the magnetic screening. On the other hand, the amplitude of oscillation in the screening response is governed by the intervortex repulsive force F_I, which renders the vortex lattice less compressible at matching fields when each vortex is surrounded by a vortex at each neighboring site. Since the repulsive force between two vortices in neighboring antidots is given by $F_I \sim \frac{\Phi_0^2}{4\pi\mu_0\Lambda a}$, $F_I/F \sim (\xi_{GL}/a)$ [15]. From the usual GL relation $\xi_{GL} \propto (1-\frac{T}{T_c})^{-1/2}$, we expect this ratio to decrease by 30% in the same temperature range, thereby making the oscillations less pronounced. We observe that at 1.45 K only the first matching field is clearly visible. Thus in the rest of the paper we concentrate primarily on the behavior around the first matching field.

The central result of this paper, namely, the screening response as a function of I_{ac} (for constant H), is shown in Fig. 3. Figure 3(a) shows M' and $-M''$ as a function of I_{ac} at 1.7 K and $H = H_M$. At low I_{ac} both M' and $-M''$ vary smoothly. However, at $I_{ac} \sim 8.8$ mA, both M' and $-M''$ exhibit a sharp jump, followed by a series of further jumps at higher excitation currents. The VME associated with these jumps becomes apparent when we compare similar measurements performed at different H. Figure 3(b) shows the variation of $-M''$ as a function I_{ac} measured at different H between 1.18 and 4 kOe. We observe that the I_{ac} at which the first jump occurs is strongly dependent on the magnetic field: The jump occurs

at the smallest value of I_{ac} when $H \approx H_m$ and shifts to higher values as one moves away from H_m. Finally, with an increase in temperature, the sharp jumps are gradually smeared, and only a smooth variation is seen above 2 K [Fig. 3(c)].

To understand the origin of these jumps, we note that for low I_{ac}, the induced $\boldsymbol{J}_S^{ac}(\boldsymbol{r})$ will cause small alternating compression and rarefaction of the VL, similar to the elastic response of a solid under oscillating stress. The gradual change in M' and $-M''$ in this regime reflects the anharmonicity of the pinning potential. As I_{ac} is increased to a critical value, for some range of r, $J_S^{ac}(r)$ will reach the critical current density J_c and the vortices in this region will get delocalized from the antidot. Above this value (which we denote as I_{ac}^p) within a circular annulus towards the periphery of the sample, the VL will start sliding over the antidot array. Thus the sharp increase in M' signifies the threshold where the elastic continuity of the VL is destroyed by the sliding. Since each hop of a vortex from one antidot to the next will induce a 2π phase slip in the intervening superconducting barrier, such a sliding motion will also cause the dissipation ($-M''$) to abruptly increase. The subsequent jumps in M' and $-M''$ with increasing I_{ac} can be understood as follows: At I_{ac}^p the vortex lattice over a circular annulus will slide back and forth over one lattice constant a of the antidot array in each cycle of ac excitation. However, as I_{ac} is increased, two events will occur. First, the circular annulus over which the vortices are delocalized will gradually increase. Second, the amplitude of the oscillatory displacement of the vortices will increase. Thus subsequent jumps correspond to the excitation current values (denoted as $I_{ac}^1, I_{ac}^2, \ldots$) where VL starts to slide over the higher integral multiples of the lattice constant ($2a, 3a, \ldots$). Also, it is interesting to note that the dissipative response shows shallow minima in between successive jumps. This shows that in addition to the uniform motion of the VL, other mechanisms of strain relaxation not involving the entire delocalized VL region, such as sliding of vortices in one domain of the antidot over another, creating lines of doubly occupied antidots, or the fracture of the VL into disconnected icebergs of VL domains, might also be playing a role. This is also responsible for the successive jumps to be gradually smaller in magnitude.

We now investigate whether the jump at I_{ac}^p can be understood in terms of conventional depinning of vortices from the underlying antidot array. For this, we need to compare the depinning force (F_p) for an isolated vortex to overcome the pinning by an antidot with the force exerted on a vortex by the supercurrent (F_{ac}^c) at $J_S^{ac} \sim J_c$. We first calculate $J_S^{ac}(r)$ for the geometry of our coil and the sample. This can in principle be done by numerically solving the Maxwell equations and the London equation using the scheme outlined in Ref. [22], by replacing the London penetration depth with the Campbell penetration depth [23,24] λ_p. However, here λ_p is itself a function of J_S^{ac}, approximately following the semiempirical relation [25] $\lambda_p(J_S^{ac}) = \frac{\lambda_p(0)}{(1-J_S^{ac}/J_c)^{1/4}}$. Therefore, to calculate $J_S^{ac}(r)$ we adopt the following iterative procedure. Since $\lambda_p(J_S^{ac}) \approx \lambda_p(0)$ for $J_S^{ac} \ll J_c$, we use the value of M' measured with $I_{ac} = 1$ mA $\ll I_{ac}^p$ [for which $J_S^{ac}(r) \ll J_c$ over the entire sample] to obtain [26] $\lambda_p(0) \approx 3100$ nm. Using this value of $\lambda_p(0)$ and a trial value of J_c, we incorporate the $J_S^{ac}(r)$ dependence of λ_p for higher values of I_{ac} and

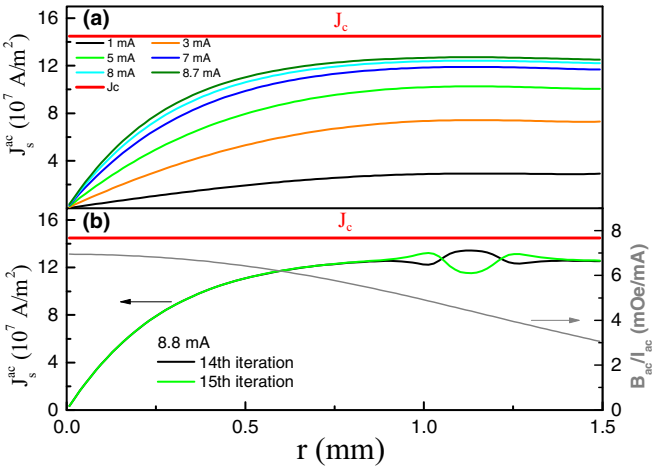

FIG. 4. (a) Simulated value of J_S^{ac} along the radius of the film for $I_{ac} \sim 1-8.7$ mA. (b) Simulated value of J_S^{ac} along the radius of the films for $I_{ac} \sim 8.8$ mA for the 14th and 15th iteration cycle; here, the simulation does not converge to a unique value and the solution becomes bistable. The profile of the ac magnetic field (B_{ac}) arising from the primary coil is shown in the same panel.

obtain a self-consistent current profile (see the Supplemental Material [27]). $J_S^{ac}(r)$ increases linearly with r for small r and saturates beyond $r > 0.9$ mm, as shown in Fig. 4(a). As I_{ac} is increased, this saturation current reaches J_c at some critical I_{ac}, beyond which the iterative procedure fails to converge to a unique profile [Fig. 4(b)]. This critical value $I_{ac} \approx I_{ac}^p$, where the VL on the outer annulus of the film ($r \gtrsim 0.9$ mm) starts sliding over the antidot array. The variational J_c for our film is then chosen so that I_{ac}^p is matched with the experimentally observed I_{ac}^p. This procedure yields $J_c \sim 1.2-1.4 \times 10^8$ A/m^2 at the first matching field for our sample, where the uncertainty is given by the difference between the maximum $J_S^{ac}(r)$ for which we obtain a stable solution and the trial J_c value. Therefore, the force exerted on a single vortex for $J_S^{ac} \sim J_c$ is $F_{ac}^c = J_c \Phi_0 t \sim 6.4 - 7.5 \times 10^{-15}$ N. To estimate F_p, we note that the confining potential created by the superconductor surrounding an antidot can be obtained from the vortex energy calculated in a thin film superconducting strip [28,29], i.e., $E(r) = \frac{\Phi_0^2}{2\pi\mu_0\Lambda} \ln[\frac{2w}{\pi\xi_{GL}} \sin(\frac{\pi(r-\frac{d}{2})}{w})]$, where $\Lambda(=2\lambda^2/t)$ is the Pearl's penetration depth, w is the width of the superconductor separating two antidots, and μ_0 is the vacuum permeability. This relation is valid when the core of the vortex is completely inside the superconductor, i.e., $r > 2\xi_{GL} + d/2$. The form of the potential implies that the restoring force on the vortex will monotonically decrease as the vortex position is changed from the edge towards the center of the superconducting strip. Thus the depinning force is given by $F_p = \frac{\partial E}{\partial r}|_{r\sim(2\xi_{GL}+\frac{d}{2})} \sim \frac{\Phi_0^2}{4\pi\mu_0\Lambda\xi_{GL}} = 4.41 \times 10^{-14}$ N, where $\xi_{GL} \sim 8$ nm [17], which is one order of magnitude larger than F_{ac}^c. This difference cannot be accounted for by the thermally activated hopping of vortices from the following energetic consideration. The potential barrier a vortex has to overcome to hop from one antidot to the adjacent one is given by

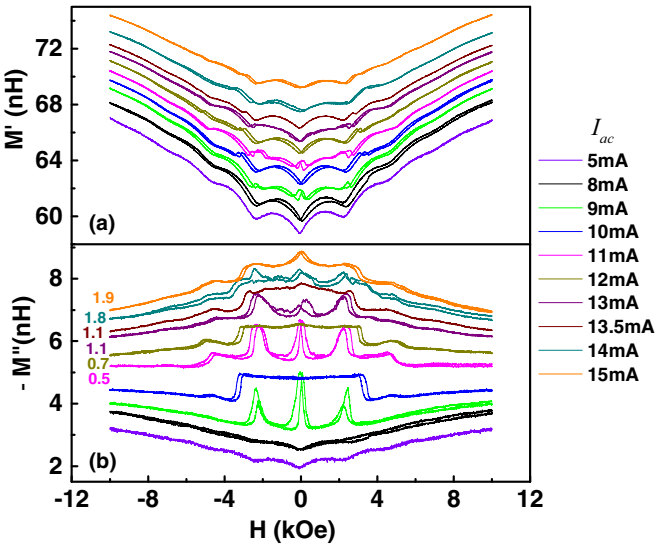

FIG. 5. (a) $M'-H$ and (b) $-M''-H$ at different I_{ac} at 1.7 K. The values of I_{ac} correspond to the vertical dashed arrows shown in Fig. 3(a). The data are recorded by sweeping H from 10 to -10 kOe and back. A small hysteresis between positive and negative field sweeps is observed in all curves. In (b) some of the curves have been shifted upward for clarity, by an amount mentioned next to the curve.

$E(r)|_{\max} = \frac{\Phi_0^2}{2\pi\mu_0\Lambda}\ln(\frac{2w}{\pi\xi_{GL}}) \sim 7$ meV. On the other hand, at 1.7 K, $k_BT \sim 0.15$ meV, such that thermally activated hopping will play a negligible role. Therefore, the delocalization of the vortices at I_{ac}^p is clearly a collective phenomenon driven by an interplay of the intervortex interaction and localization [30].

We now focus on the role of VME on I_{ac}^p. I_{ac}^p is lowest for $H \approx H_m$ when the VL is the most rigid. Physically, this can be understood from the fact that the delocalization of vortices is governed both by the individual pinning potential of the antidot and the intervortex interaction. Away from the matching field the antidot array either contains some empty sites (for $H < H_M$) or sites that are doubly occupied by vortices (for $H > H_m$) which can accommodate the change of flux through a local rearrangement of vortices without breaking the overall elastic continuity. Thus the VL gets collectively delocalized only when these local rearrangements become energetically unfavorable compared to the sliding of the entire VL. In contrast, at H_m where each antidot is filled with exactly one vortex, any such local rearrangement will trigger a collective delocalization of the entire VL. Subsequent thresholds I_{ac}^1 and I_{ac}^2 also show a similar variation with H, governed by a similar energetic consideration.

It is now instructive to look at the evolution of M' and M'' with H for different I_{ac}. Figures 5(a) and 5(b) show $M'-H$ and $(-M'')-H$ at 1.7 K corresponding to I_{ac} values marked by the vertical dashed arrows in Fig. 3(a), while the magnetic field is swept from 10 to -10 kOe and back. For $I_{ac} < I_{ac}^p \sim 8.8$ mA, $M'-H$ traces remain qualitatively similar, and display minima at the matching fields. $(-M'')-H$ also displays shallow dips at the matching field. Both of these are consistent with the elastic regime, where the VL becomes more rigid at H_m and therefore each vortex oscillates with a smaller amplitude. Since no vortex hop is involved in this range, $-M''$ is dominated by the Bardeen-Stephen dissipation due to the oscillating vortex in the superconducting region surrounding every antidot. This behavior drastically changes at $I_{ac} = 9$ mA $\sim I_{ac}^p$. Here, M' develops small peaks at H_m, showing that the VL gets delocalized at the matching field. This leaves a pronounced signature in the dissipative response and $-M''$ exhibits pronounced peaks at $H = H_m$. However, since this excitation cannot delocalize the VL away from the matching field, the elastic response is restored as we move away from H_m. As I_{ac} is increased to 10 mA (midway between I_{ac}^p and I_{ac}^1), the vortices are delocalized even away from H_m and the peaks in M' shift to higher fields. At the same field, $-M''$ shows an abrupt jump. Interestingly, below the delocalization field, M' shows minima at H_m, characteristic of the elastic response of the VL, whereas $-M''$ remains flat and featureless. To understand this difference, we note that when the outer annulus of the VL gets decoupled from the antidot array, the central region continues to behave as an elastic solid. This elastic core will contribute to exhibit a matching effect in M' whereas the outer region sliding over the antidot array will contribute a nearly field independent background. On the other hand, since the central elastic core will contribute very little to dissipation, $-M''$ will be dominated by the delocalized portion of the VL in the outer annulus. The nearly constant $-M''$ shows that at this excitation the VL in the outer annular region remains delocalized over the entire range of fields between $H = \pm H_m$. We observe that this qualitative behavior repeats between I_{ac}^1 and I_{ac}^2, and I_{ac}^2 and I_{ac}^3, though the matching effect in M' becomes progressively weaker as a larger fraction of the VL gets delocalized.

One interesting aspect of our data is the behavior at $H = 0$. The zero field minimum in M' also transforms into a small peak with an increase in I_{ac}, similar to the first matching field, which is unexpected if we consider the antidot array to be empty. In fact, $-M' - I_{ac}$ also shows characteristic jumps [26] at $H = 0$ though the structure is more complex than at $H = H_m$. The most likely explanation for this observation is that the zero field state is not empty but is populated with vortex and antivortex pairs in the antidot array, which are expected to spontaneously form in a 2D superconductor. These vortex-antivortex pairs can also get delocalized under ac excitation, but its dynamics will be much more complex owing to the possibility of vortex-antivortex annihilation by the excitation field, and is currently not captured within our model. The existence of vortex-antivortex pairs in zero field in an antidot array has also been conjectured in an earlier study investigating the transport current-stimulated depinning [14] of the VL, where the zero field state exhibited a behavior similar to that at matching fields.

IV. SUMMARY AND OUTLOOK

In summary, we have shown that the Mott-like state of the VL realized in superconducting films with an antidot array (where each vortex is localized in an antidot) transforms at a characteristic ac magnetic field excitation to a metal-like state where the vortices are delocalized. This transformation happens well below the conventional depinning threshold and shows a pronounced VME, confirming that it is a collective phenomenon governed both by the strength of the individual

pinning centers and the intervortex interactions. From this standpoint, our experimental observation is analogous to the dynamical vortex Mott insulator-to-metal transition induced by a transport current reported in Ref. [13]. However, in our case, further investigations are required to understand whether this represents a true dynamical phase transition and why the characteristic jumps in M associated with this transition disappear well below T_c.

It is also interesting to note in this context, that our observation that I_{ac}^{p} (and hence J_c) is lowest at the matching field, is different from the variation of critical current very close to T_c [5], where the critical current was reported to show maxima at the matching field. The origin of this difference can be traced to Little-Parks-like quantum interference (QI) effects [31,32]. When the width of the superconductor (w) in the antidot array is smaller than ξ_{GL}, QI causes the supercurrent around each loop to go to zero at the matching fields. Thus the amplitude of the superconducting order parameter which follows the variation in supercurrent gets enhanced at the matching field, which in turn reflects as maxima [33] in T_c and the critical current. Therefore, QI will produce an effect opposite to VME on the critical current. Since ξ_{GL} diverges close to T_c, QI will always dominate at these temperatures and give rise to maxima in the critical current at the matching fields. In contrast, our experiments are carried out at low temperatures where $\xi_{GL} \ll w$, and QI plays an insignificant role. Therefore, in addition to avoiding the effect of thermally excited vortex motion, our experiments are significant from the standpoint that they allow us to look at a VME that is uncontaminated by QI.

ACKNOWLEDGMENTS

We thank Valerii Vinokur for critically reading the paper and for explaining the connection between our results and the Mott-vortex-to-metal transition. We thank Bhagyashree A. Chalke and Rudheer Bapat for help with the scanning electron microscopy measurements. R.S. acknowledges useful discussions with Ahana Chakraborty. P.R. acknowledges the Department of Atomic Energy, Government of India, and Science and Engineering Research Board, Government of India for financial support (Grant No. EMR/2015/000083). S.B. acknowledges partial financial support from the Department of Science and Technology, India through Grants No. SERB/F/1877/2012 and No. SERB/F/745/2014 and the Indian National Science Academy through Grant No. SP/YSP/73/2012/1875.

[1] M. J. Higgins and S. Bhattacharya, Varieties of dynamics in a disordered flux-line lattice, Physica C **257**, 232 (1996).

[2] E. H. Brandt, The flux-line lattice in superconductors, Rep. Prog. Phys. **58**, 1465 (1995).

[3] V. V. Moshchalkov, M. Baert, V. V. Metlushko, E. Rosseel, M. J. Van Bael, K. Temst, Y. Bruynseraede, and R. Jonckheere, Pinning by an antidot lattice: The problem of the optimum antidot size, Phys. Rev. B **57**, 3615 (1998).

[4] U. Welp, Z. L. Xiao, J. S. Jiang, V. K. Vlasko-Vlasov, S. D. Bader, G. W. Crabtree, J. Liang, H. Chik, and J. M. Xu, Superconducting transition and vortex pinning in Nb films patterned with nanoscale hole arrays, Phys. Rev. B **66**, 212507 (2002).

[5] A. V. Silhanek, L. Van Look, R. Jonckheere, B. Y. Zhu, S. Raedts, and V. V. Moshchalkov, Enhanced vortex pinning by a composite antidot lattice in a superconducting Pb film, Phys. Rev. B **72**, 014507 (2005).

[6] W. Vinckx, J. Vanacken, V. V. Moshchalkov, S. Matefi-Tempfli, M. Matefi-Tempfli, S. Michotte, and L. Piraux, Vortex pinning in superconducting Nb thin films deposited on nanoporous alumina templates, Eur. Phys. J. B **53**, 199 (2006).

[7] A. D. Thakur, S. Ooi, S. P. Chockalingam, J. Jesudasan, P. Raychaudhuri, and K. Hirata, Vortex matching effect in engineered thin films of NbN, Appl. Phys. Lett. **94**, 262501 (2009).

[8] G. R. Berdiyorov, M. V. Milošević, and F. M. Peeters, Vortex configurations and critical parameters in superconducting thin films containing antidot arrays: Nonlinear Ginzburg-Landau theory, Phys. Rev. B **74**, 174512 (2006).

[9] D. R. Nelson and V. M. Vinokur, Boson localization and correlated pinning of superconducting vortex arrays, Phys. Rev. B **48**, 13060 (1993).

[10] K. Harada, O. Kamimura, H. Kasai, T. Matsuda, A. Tonomura, and V. V. Moshchalkov, Direct observation of vortex dynamics in superconducting films with regular arrays of defects, Science **274**, 1167 (1996).

[11] M. Baert, V. V. Metlushko, R. Jonckheere, V. V. Moshchalkov, and Y. Bruynseraede, Composite Flux-Line Lattices Stabilized in Superconducting Films by a Regular Array of Artificial Defects, Phys. Rev. Lett. **74**, 3269 (1995).

[12] S. Goldberg, Y. Segev, Y. Myasoedov, I. Gutman, N. Avraham, M. Rappaport, E. Zeldov, T. Tamegai, C. W. Hicks, and K. A. Moler, Mott insulator phases and first-order melting in $Bi_2Sr_2CaCu_2O_{8+\delta}$ crystals with periodic surface holes, Phys. Rev. B **79**, 064523 (2009).

[13] N. Poccia, T. I. Baturina, F. Coneri, C. G. Molenaar, X. R. Wang, G. Bianconi, A. Brinkman, H. Hilgenkamp, A. A. Golubov, and V. M. Vinokur, Critical behavior at a dynamic vortex insulator-to-metal transition, Science **349**, 1202 (2015).

[14] Z. Jiang, D. A. Dikin, V. Chandrasekhar, V. V. Metlushko, and V. V. Moshchalkov, Pinning phenomena in a superconducting film with a square lattice of artificial pinning centers, Appl. Phys. Lett. **84**, 5371 (2004).

[15] S. Kumar, C. Kumar, J. Jesudasan, V. Bagwe, P. Raychaudhuri, and S. Bose, A two-coil mutual inductance technique to study matching effect in disordered NbN thin films, Appl. Phys. Lett. **103**, 262601 (2013).

[16] S. Kumar, C. Kumar, J. Jesudasan, V. Bagwe, P. Parab, P. Raychaudhuri, and S. Bose, Origin of matching effect in anti-dot array of superconducting NbN thin films, Supercond. Sci. Technol. **28**, 055007 (2015).

[17] M. Mondal, M. Chand, A. Kamlapure, J. Jesudasan, V. C. Bagwe, S. Kumar, G. Saraswat, V. Tripathi, and P. Raychaudhuri, Phase diagram and upper critical field of homogeneously

disordered epitaxial 3-dimensional NbN films, J. Supercond. Novel Magn. **24**, 341 (2011).

[18] M. Mondal, A. Kamlapure, M. Chand, G. Saraswat, S. Kumar, J. Jesudasan, L. Benfatto, V. Tripathi, and P. Raychaudhuri, Phase Fluctuations in a Strongly Disordered s-Wave NbN Superconductor Close to the Metal-Insulator Transition, Phys. Rev. Lett. **106**, 047001 (2011).

[19] M. Chand, G. Saraswat, A. Kamlapure, M. Mondal, S. Kumar, J. Jesudasan, V. Bagwe, L. Benfatto, V. Tripathi, and P. Raychaudhuri, Phase diagram of a strongly disordered s-wave superconductor, NbN, close to the metal-insulator transition, Phys. Rev. B **85**, 014508 (2012).

[20] The Fourier transform is obtained by using the image processing module of WSXM software: I. Horcas, R. Fernández, J. M. Gómez-Rodríguez, J. Colchero, J. Gómez-Herrero, and A. M. Baro, WSXM: A software for scanning probe microscopy and a tool for nanotechnology, Rev. Sci. Instrum. **78**, 013705 (2007).

[21] See Supplemental Material at http://link.aps.org/supplemental/10.1103/PhysRevB.95.054513, Sec. III, for a more detailed discussion on the magnetic field variation of M'.

[22] S. J. Turneaure, E. R. Ulm, and T. R. Lemberger, Numerical modeling of a two-coil apparatus for measuring the magnetic penetration depth in superconducting films and arrays, J. Appl. Phys. **79**, 4221 (1996).

[23] A. M. Campbell, The response of pinned flux vortices to low-frequency fields, J. Phys. C: Solid State Phys. **2**, 1492 (1969).

[24] E. H. Brandt, Penetration of Magnetic ac Fields into Type-II Superconductors, Phys. Rev. Lett. **67**, 2219 (1991).

[25] R. Prozorov, R. W. Giannetta, N. Kameda, T. Tamegai, J. A. Schlueter, and P. Fournier, Campbell penetration depth of a superconductor in the critical state, Phys. Rev. B **67**, 184501 (2003).

[26] The procedure for obtaining λ from M' is outlined in Ref. [21]. See also M. Mondal, Phase fluctuations in a conventional s-wave superconductor: Role of dimensionality and disorder, arXiv:1303.7396.

[27] See Supplemental Material at http://link.aps.org/supplemental/10.1103/PhysRevB.95.054513, Sec. I, for details of the computational procedure for obtaining $J_s^{\rm ac}(r)$. Section II shows a comparison of $-M''$ as a function of $I_{\rm ac}$ at $H = 0$ and $H = H_m$.

[28] V. G. Kogan, Pearl's vortex near the film edge, Phys. Rev. B **49**, 15874 (1994).

[29] J. R. Kirtley, C. C. Tsuei, V. G. Kogan, J. R. Clem, H. Raffy, and Z. Z. Li, Fluxoid dynamics in superconducting thin film rings, Phys. Rev. B **68**, 214505 (2003).

[30] See Supplemental Material at http://link.aps.org/supplemental/10.1103/PhysRevB.95.054513, Sec. IV. The same conclusion can be arrived at by considering the upper bound of the vortex displacement due to the ac magnetic field.

[31] W. A. Little and R. D. Parks, Observation of Quantum Periodicity in the Transition Temperature of a Superconducting Cylinder, Phys. Rev. Lett. **9**, 9 (1962).

[32] Y.-L. Lin and F. Nori, Quantum interference in superconducting wire networks and Josephson junction arrays: An analytical approach based on multiple-loop Aharonov-Bohm Feynman path integrals, Phys. Rev. B **65**, 214504 (2002).

[33] M. J. Higgins, Y. Xiao, S. Bhattacharya, P. M. Chaikin, S. Sethuraman, R. Bojko, and D. Spencer, Superconducting phase transitions in a kagomé wire network, Phys. Rev. B **61**, R894(R) (2000).